

# UCSF

## UC San Francisco Previously Published Works

### Title

New insights into human female reproductive tract development

### Permalink

<https://escholarship.org/uc/item/7pm5800b>

### Authors

Robboy, Stanley J  
Kurita, Takeshi  
Baskin, Laurence  
et al.

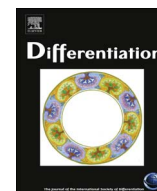
### Publication Date

2017-09-01

### DOI

10.1016/j.diff.2017.08.002

Peer reviewed



# New insights into human female reproductive tract development



Stanley J. Robboy<sup>a,\*</sup>, Takeshi Kurita<sup>b</sup>, Laurence Baskin<sup>c</sup>, Gerald R. Cunha<sup>c</sup>

<sup>a</sup> Department of Pathology, Duke University, Davison Building, Box 3712, Durham, NC 27710, United States

<sup>b</sup> Department of Cancer Biology and Genetics, The Comprehensive Cancer Center, Ohio State University, 460 W. 12th Avenue, 812 Biomedical Research Tower, Columbus, OH 43210, United States

<sup>c</sup> Department of Urology, University of California, 400 Parnassus Avenue, San Francisco, CA 94143, United States

## ARTICLE INFO

### Keywords:

Human Müllerian duct  
Urogenital sinus  
Uterovaginal canal  
Uterus  
Cervix  
Vagina

## ABSTRACT

We present a detailed review of the embryonic and fetal development of the human female reproductive tract utilizing specimens from the 5th through the 22nd gestational week. Hematoxylin and eosin (H & E) as well as immunohistochemical stains were used to study the development of the human uterine tube, endometrium, myometrium, uterine cervix and vagina. Our study revisits and updates the classical reports of Koff (1933) and Bulmer (1957) and presents new data on development of human vaginal epithelium. Koff proposed that the upper 4/5ths of the vagina is derived from Müllerian epithelium and the lower 1/5th derived from urogenital sinus epithelium, while Bulmer proposed that vaginal epithelium derives solely from urogenital sinus epithelium. These conclusions were based entirely upon H & E stained sections. A central player in human vaginal epithelial development is the solid vaginal plate, which arises from the uterovaginal canal (fused Müllerian ducts) cranially and squamous epithelium of urogenital sinus caudally. Since Müllerian and urogenital sinus epithelium cannot be unequivocally identified in H & E stained sections, we used immunostaining for PAX2 (reactive with Müllerian epithelium) and FOXA1 (reactive with urogenital sinus epithelium). By this technique, the PAX2/FOXA1 boundary was located at the extreme caudal aspect of the vaginal plate at 12 weeks. During the ensuing weeks, the PAX2/FOXA1 boundary progressively extended cranially such that by 21 weeks the entire vaginal epithelium was FOXA1-reactive and PAX2-negative. This observation supports Bulmer's proposal that human vaginal epithelium derives solely from urogenital sinus epithelium. Clearly, the development of the human vagina is far more complex than previously envisioned and appears to be distinctly different in many respects from mouse vaginal development.

## 1. Introduction

The development of the human female reproductive tract and especially knowledge concerning the germ cell layer derivation of vaginal epithelium rests on histological, histochemical observations and to limited, immunohistochemical investigations. The seminal paper on this topic by Koff appeared in 1933 when the technical state of the art was tissue sections 25–100  $\mu$  thick stained with hematoxylin and eosin (Koff, 1933). From this humble beginning, the field has progressed to elegant epithelial cell lineage tracing to reveal the relative contribution of epithelium of the urogenital sinus (UGS) versus the Müllerian (paramesonephric) ducts to vaginal epithelial development in mice (Kurita, 2010) and immunohistochemical studies in man (Fritsch et al., 2013, 2012). The current paper and its two companions (a) review the collective trove on human female reproductive tract development (Bulmer, 1957; Cai, 2009; Forsberg, 1996, 1973; Fritsch

et al., 2013, 2012; Hunter, 1930; Koff, 1933; Konishi et al., 1984; Kurita, 2010; Mutter and Robboy, 2014; O'Rahilly, 1977, 1983; O'Rahilly and Muller, 1992; Reich and Fritsch, 2014; Sinisi et al., 2003; Sulak et al., 2007), (b) provide new data on the derivation of human vaginal epithelium and (c) highlight the role of differentiation markers and signaling pathways involved in human uterovaginal development.

Both the male and female reproductive tracts collectively consist of the gonads, their internal ductal systems, and the external genitalia. The embryonic anlagen for these elements appear during the first trimester, followed by extensive growth and maturation during the fetal period and postnatally. Ovarian development occurs in fetuses with the XX chromosome pair, while testicular development occurs in fetuses with XY chromosomes. This review focuses on the developing female internal genitalia (uterine tube, uterine body, cervix, and vagina). It omits discussion of the molecular genetic basis of both normal (Mutter

Abbreviations: H & E, hematoxylin & eosin; UGS, urogenital sinus; MDE, Müllerian duct epithelium; UGE, urogenital sinus epithelium

\* Corresponding author.

E-mail address: [stanley.robboy@duke.edu](mailto:stanley.robboy@duke.edu) (S.J. Robboy).

<http://dx.doi.org/10.1016/j.diff.2017.08.002>

Received 8 June 2017; Received in revised form 31 July 2017; Accepted 1 August 2017

Available online 11 August 2017

0301-4681/ © 2017 Published by Elsevier B.V. on behalf of International Society of Differentiation.

**Table 1**  
Normal development of the Müllerian and its derivatives <sup>a</sup>.

Week of gestationpost ovulation	Crown-rump (mm)	Heel-toe length (mm)	Carnegie Stage	Developmental event
3 wk	2.5 mm			Pronephric tubules form; pronephric (mesonephric) duct arises and grows caudad.
4 wk	3–5 mm		Stage 12	Pronephros degenerated, but mesonephric duct reaches cloaca.
5 wk	7 mm			
6 wk	11 mm		Stage 17	Müllerian ducts appear as funnel-shaped opening of celomic epithelium.
7 wk	18 mm		Stage 22	Müllerian ducts migrate to about half distance to urogenital sinus.
	23 mm		Stage 23	Müllerian ducts extend caudally to near the urogenital sinus.
8 wk	30 mm		30 mm	Müllerian ducts begin midline fusion and make contact with urogenital sinus at the Müllerian tubercle.
	36 mm			
9 wk	50 mm		56 mm	Müllerian ducts fuses (entire septum gone); Epithelium lining uterovaginal canal stratifies (1–2 cells layers thick).
10 wk	60 mm	2–5 mm	60 mm	
11 wk	71 mm	5–8 mm	63 mm	Bilateral sinovaginal bulbs (evagination of UGS) appear.
	75 mm		75 mm	Vaginal plate first seen distinctly at 75 mm (complete at 140 mm; week 17).
12 w	93 mm	8–11 mm		
13 wk	105 mm	12–14 mm	100 mm	
14 wk	110–140 mm116 mm	15–17 mm	110–140 mm	Marked growth of caudal vagina (between 110 & 140 mm).
			130 mm	Vaginal rudiment reaches level of vestibular glands; uterovaginal canal (15 mm total length) divisible into vagina (one-half), cervix (one-third), and corpus (one-sixth); boundaries ill defined.
				Endometrial stromal & myometrial layers of uterus become apparent.
				Solid epithelial anlage of anterior and posterior fornices appear
15 wk	130 –140 mm	18–21 mm	135 mm	Vagina begins to show slight estrogen (epithelial squamous differentiation)
			139 mm	Cervix about 5 mm long
			140 mm	Uterine (Fallopian) tube begins active growth phase
16 wk	142 mm	21–24 mm		Vaginal plate extends from vestibule to endocervical canal.
			151 mm	Uterine/cervical glands begin as outpouchings of simple columnar epithelium
			151 mm	Vaginal plate longest and begins to canalize.
				Solid epithelial projections of anterior and posterior fornices demarcate cranial end of vagina.
17 wk	153–162 mm	24–27 mm	160 mm	Palmate folds of cervix appear (forerunner adult cervix).
			162 mm	Mucoid development of cervix begins. Estrogen-induced thickening of vaginal epithelium.
18 wk	164 mm	27–30 mm	170 mm	Fornices hollow.
19 wk	177 mm	31–33 mm	180 mm	Cavitation of vaginal canal completed.
			185 mm	Uterine tube growth marked (~3 mm/week to week 34).
			190 mm	Cervix about 10 mm long.
21 wk	197 mm	37–40 mm		
22 wk	208 mm	40–43 mm	200 mm	Vagina completely formed.
			210 mm	Differentiation of muscular layer of uterus complete.
			227 mm	
24 wk	215–295	47–49 mm		Uterine fundus well defined; uterus assumes adult form. Uterine body about 10 mm long.
25 wk	227			
26 wk	240			Cervix about 20 mm long.
34 wk	305			Cervix about 25 mm long.
38 wk	362 mm			Birth.

NOTE: Week 1 includes = days 1–7, week 2 = days 7–14, etc.  
<sup>a</sup> Table compiled from Koff (1933), Mutter and Robboy (2014), O’Rahilly (1977, 1983), O’Rahilly and Muller (1992, 2010).

**Table 2**  
Definition of terms referred to in human and mouse vaginal development.

Human terms	Definition
Uterovaginal canal (Koff, 1933)	The fused Müllerian ducts located in the pelvic midline.
Müllerian tubercle (Fritsch et al., 2013; Koff, 1933)	The Müllerian tubercle is the initial point of contact of the Müllerian ducts and with the UGS.
Sinovaginal bulb (Koff, 1933; Shapiro et al., 2000)	Cranial expansion of urogenital sinus epithelium that contributes to the vaginal plate
Vaginal plate (Koff, 1933)	A solid epithelial plate in the caudal uterovaginal canal
<b>Mouse terms</b>	
Müllerian vagina (Kurita, 2011)	The cranial portion of the perinatal mouse vagina. The epithelium, which transforms from simple columnar to stratified squamous, is derived from the fused Müllerian ducts
Sinus vagina (Kurita, 2011)	A solid dorsal process of the urogenital sinus that joins with the Müllerian vagina.

and Robboy, 2014) and abnormal gonadal sexual determination and the developing gonads themselves (Robboy and Mutter, 2014). Accordingly, this article summarizes knowledge of how female internal genitalia develop from their initial appearance in about week five through parturition (Table 1). The first of two companion articles amplifies the immunohistochemical changes that occur during human

**Table 3**  
Human fetal specimens.

Code #	Heel-toe length	Gestational age	Analysis
AC341	3.5 mm	8	Gross
AC413	6 mm	9	H & E
AC353	6.5 mm	9	Gross
AC339	8 mm	10wks	Gross
AC356	9 mm	10wks	Gross
AC418	9 mm	9wks	Gross
AC454	9 mm	9wks	H & E, IHC
AC428	9 mm	9wks	H & E, IHC
AC476	9.5 mm	9.5wks	H & E, IHC
AC360	8 mm	10wks	Gross
AC275	8 mm	10wks	Gross
AC447	9.5 mm	9/5	H & E, IHC
AC81	11 mm	11wks	H & E, IHC
AC151	11.2 mm	11wks	H & E, IHC
AC307	11 mm	11wks	Gross
AC448	11 mm	11wks	H & E, IHC
AC209	12 mm	12wks	H & E, IHC
AC261	10 mm	12.5wks	H & E, IHC
AC251	10 mm	12wks	H & E, IHC
AC452	15 mm	12wks	Gross
AC375	16 mm	12wks	H & E, IHC
AC247	12 mm	13wks	H & E, IHC
AC121	13 mm	13wks	Gross, H & E, IHC
AC122	12 mm	13wks	Gross, H & E, IHC
AC335	18 mm	13wks	Gross
AC323	20 mm	13wks	Gross
AC260	13 mm	13.3wks	H & E, IHC
AC288	18 mm	13wks	Gross
AC449	18 mm	13wks	Gross
AC113	17.5 mm	13wks	Gross, H & E
AC119	20 mm	13wks	H & E, IHC
AC150	19 mm	13wks	H & E, IHC
AC159	17 mm	14wks	H & E, IHC
AC296	22 mm	14wks	Gross
AC362	20 mm	14wks	Gross
AC455	23 mm	14wks	H & E, IHC
AC345	25 mm	14wks	H & E
AC479	22 mm	14wks	Gross
AC355	23 mm	14wks	H & E, IHC
AC289	25 mm	15wks	Gross
AC491	24 mm	15wks	H & E, IHC
AC297	25 mm	15wks	Gross
AC358	26 mm	15wks	Gross
AC258	22 mm	16wks	H & E, IHC
AC327	27 mm	16wks	H & E, IHC
AC445	27 mm	16wks	H & E, IHC
AC508	36 mm	18wks	H & E, IHC
AC503	34 mm	18wks	H & E, IHC
AC357	37 mm	19wks	Gross
AC337	37 mm	19wks	Gross
AC269	32 mm	19wks	Gross
AC165	34 mm	20wks	H & E, IHC
AC312	40 mm	20wks	Gross
AC510	44 mm	21wks	H & E, IHC
AC461	45 mm	21wks	H & E, IHC
AC303	46 mm	22wks	Gross
AC158	57 mm	24wks	H & E

female reproductive tract development (Cunha et al., in press(a)). The second companion paper presents our xenografting and tissue recombinants experiments that will help explain the underlying developmental principles of female reproductive tract morphogenesis in both man and mouse (Cunha et al., in press(b)). Our discussion of vaginal development will also compare and contrast the mouse and human, and for this purpose it is essential to recognize the different terminology used historically in human versus mouse female reproductive tract development (Table 2).

## 2. Materials and methods

Two sets of human specimens were used. The primary set relied on 48 first and second-trimester human fetal specimens collected free of patient identifiers after elective termination of pregnancy (with Committee on Human Research approval at the University of California at San Francisco, IRB# 12-08813) (Table 3). Gender was determined for most specimens by Wolffian (mesonephric) and Müllerian (paramesonephric) duct morphology; for the youngest specimens PCR of X and Y- chromosomal sequences determined sex (Li et al., 2015). A dissecting microscope was used to identify and photograph the internal genitalia. Since all aborted specimens were received disrupted, heel-toe length proved to be the only useful determinant of gestational age (Drey et al., 2005; Mercer et al., 1987; Mhaskar et al., 1989). The second set of specimens came from a larger collection of the authors from 1978 to 1982 (Robboy et al., 1982a; Taguchi et al., 1983, 1984; Cunha et al., 1987). This later collection of specimens was aged 5–17 weeks of gestation.

Gestational timing of the human embryos in the Carnegie Collection was derived from patient interviews, even though information concerning the last menstrual period is notoriously inaccurate, especially for second trimester abortions. “An embryo is assigned a Carnegie stage (numbered from 1 to 23) based on its external features. This staging system is not dependent on the chronological age or the size of the embryo. The stages are in a sense arbitrary levels of maturity based on multiple physical features. Embryos that might have different ages or sizes can be assigned the same Carnegie stage based on their external appearance because of the natural variation which occurs between individuals.” (Smith, 2016).

Historically, most abortions involved vaginal delivery of intact embryos/fetuses from which crown-rump measurements were used as a measure of embryonic/fetal age (Streeter, 1951). Today, crown-rump measurements are rarely useful as current abortion procedures disrupt overall specimen integrity. Accordingly, we have used heel-toe length as a proxy to determine fetal maturity, which gives a rough estimate of age at best. As the Carnegie Collection literature advocates, gross images ordered by increasing size and morphological complexity is more important than exact estimate of age. Accordingly, Fig. 1 provides images of a wholmount series human embryos from the Carnegie Collection (<http://embryo.soad.umich.edu/carnStages/carnStages.html>) that was useful for our youngest specimens (Fig. 2).

Human female reproductive tract specimens were sectioned serially. Every tenth section was stained with hematoxylin and eosin (H & E). Selected paraffin sections were immunostained as described previously (Rodriguez et al., 2012) with the following antibodies: PAX2

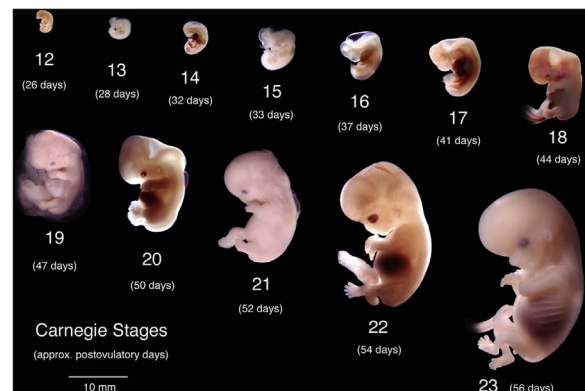


**Fig. 1.** Wholmount photos of developing human embryos from the Carnegie collection. Note increasing size and morphological complexity with developmental stage. Image from Dr. Brad Smith, University of Michigan (<http://embryo.soad.umich.edu/carnStages/carnStages.html>) NIH award N01-HD-6-3257 P/G F003637, with permission.

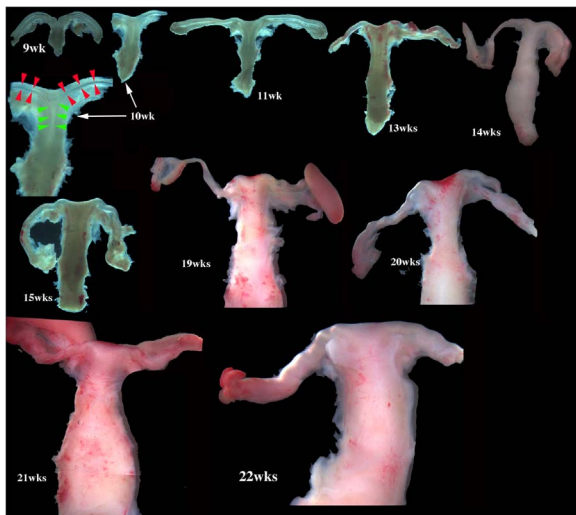


**Fig. 2.** Wholmount photos of developing human fetal female internal genitalia staged by heel-toe measurements. Note (a) increase in size and morphological complexity with time, and (b) that landmarks distinguishing the uterine corpus, cervix and vagina are subtle/non-existent. Specimens photographed with transmitted light (9, 10, 11, 13 and 15 weeks) permit visualization of internal (epithelial) organization in regions not too thick. The 10-week specimen is shown at both low and high magnifications. Red arrowheads demarcate the epithelium defining the lumen of the uterine tube. Green arrowheads define the epithelium lining the uterus. Relative sizes of specimens are not exact, but increase with age.

(Abcam, Cambridge, MA, Catalogue # ab150391, 1/50), FOXA1 (Atlas Antibodies, Bromma, Sweden, Catalogue # HPA050505, 1/500), Isl1 (Abcam, Ab20670, 1/200), Keratin 19, E.B. Lane, Institute of Medical Biology, Singapore, 1/10) and  $\alpha$ -actin (St. Louis, MO, Catalogue # A2547, 1:2000) (Rodriguez et al., 2012). Immunostaining was detected using horseradish-peroxidase-based Vectastain kits (Vector Laboratories, Burlingame, CA). Negative controls deleted the primary antibody.

### 3. Results

#### 3.1. Early Müllerian duct development (Weeks 5 to 8, the end of embryonic period)

At the start of week 5 in human female and male embryos, the coelomic epithelium invaginates on the lateral surface of the paired urogenital ridges at the third thoracic somite level (O’Rahilly, 1973). The infoldings later become the tubal abdominal ostia of the Müllerian (paramesonephric) ducts. The irregular margins of Müllerian duct ostia will form the future fimbriae of the uterine tubes (Fallopian tubes). The paired Müllerian ducts grow caudally within the urogenital ridges using the Wolffian ducts as “guide wires.” Indeed, the Wolffian duct is requisite for caudal Müllerian duct migration towards the UGS (Gruenwald, 1941; Kobayashi et al., 2005). Cranially, mesenchyme separates the Müllerian and Wolffian ducts within the urogenital ridges (Fig. 3). More caudally, only their conjoined basement membranes separate the Müllerian and Wolffian duct epithelia without any intervening mesenchyme. Even more caudally, the tip of the Müllerian duct is in direct contact with Wolffian duct epithelium without an intervening basement membrane (Fig. 3). Accordingly, it was proposed that the Wolffian duct may contribute cells to the Müllerian duct or vice versa (Frutiger, 1969). However, cell-lineage tracing experiments in mouse have definitively shown that Wolffian duct epithelium does not contribute cells to the forming Müllerian duct (Kurita, 2010).

The track of the Wolffian and Müllerian ducts in route to the UGS exhibits two gentle curves within the paired urogenital ridges that define vertical, horizontal, and vertical portions as seen in frontal view

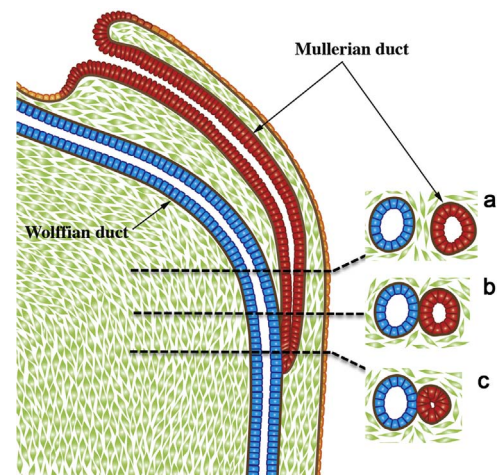


**Fig. 3.** Diagrammatic representation of the caudal growth of the Müllerian duct (MD) using the Wolffian duct (WD) as a “guide wire”. Note in (a) mesenchyme intervening between the Müllerian and Wolffian ducts, (b) contact of the basement membranes of Müllerian and Wolffian ducts, (c) direct contact of the epithelia of the Müllerian and Wolffian ducts.

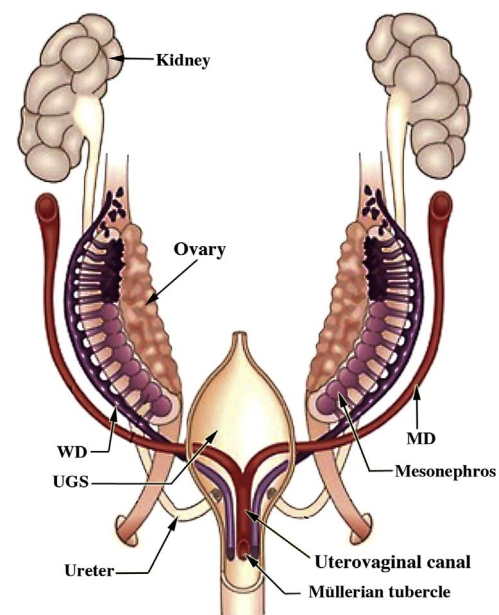


**Fig. 4.** Diagram of rudiments of human internal genitalia in the indifferent, bisexual stage (~54 days of gestation, Carnegie Stage 22). The Müllerian derivatives are red and Wolffian derivatives are purple. Note the changing anatomical relationships between the Müllerian and Wolffian ducts. Modified from Robboy et al. with permission (Robboy et al., 2002).

(Fig. 4). Accordingly, in a 54-day (Carnegie Stage 22) human embryo the bilateral urogenital ridges containing paired Wolffian and Müllerian ducts approach the midline near the urogenital sinus (Fig. 5A). The point of contact of the Müllerian ducts with the urogenital sinus, called Müllerian tubercle (Fig. 6), is controversial and poorly described and illustrated in the literature. O’Rahilly opines that the term Müllerian tubercle designating this area is unsatisfactory, stating it is “a designation as obscure as is the development of the feature in question” (O’Rahilly and Muller, 1992; O’Rahilly, 1973). He proposed “sinus tubercle” is where the epithelia of the Müllerian and Wolffian ducts (both derived from mesoderm) meet and likely mingle with endodermal epithelium of the UGS. During the 7th to 8th weeks, the right and left Müllerian ducts lie between the two Wolffian ducts as the latter approach and join into the UGS (Figs. 5B–D and 6). During the 8th week, the right and left Müllerian ducts fuse together and



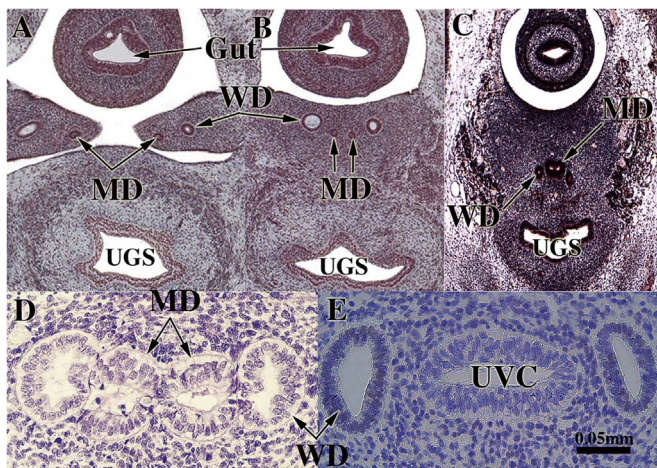


**Fig. 5.** Fusion of the Müllerian ducts to form the uterovaginal canal. (A & B) are sections of the pelvis of a stage 23 Carnegie embryo (56 days). (A) shows the urogenital ridges containing Wolffian (WD) and Müllerian ducts (MD) prior to their fusion in the midline. In (B) after midline fusion of the urogenital ridges, the paired Wolffian (WD) and Müllerian ducts (MD) are present, and the two Müllerian ducts are separated by mesenchyme. (C) is a fortuitous pelvic section of a stage 22 Carnegie embryo (54 days) demonstrating midline fusion of the right and left Müllerian ducts (MD). The midline epithelial septum is present representing the fused medial walls of the Müllerian ducts. (D) is a transverse section through the Müllerian (MD) and Wolffian ducts (WD) near their junction with the urogenital sinus. The right and left Müllerian have fused and are in direct contact without intervening basement membranes (Reprinted with permission of Robboy Associates LLC). (E) A transverse section through the uterovaginal canal with flanking Wolffian ducts (WD) of a 9-week fetus. Images (A–C) are from the Virtual Human Embryo Project (<http://virtualhumanembryo.lsuhs.edu>) with permission.

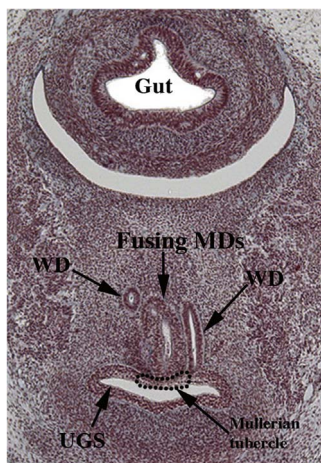


**Fig. 6.** A pelvic section of a stage 23 Carnegie embryo (56 days) showing contact of the fusing Müllerian ducts (MD) with the urogenital sinus (UGS). The point of contact of the Müllerian ducts with the urogenital sinus is called the Müllerian tubercle. Wolffian ducts (WD) also join the urogenital sinus just lateral to the Müllerian tubercle. From the Virtual Human Embryo Project (<http://virtualhumanembryo.lsuhs.edu>) with permission.

temporarily a midline epithelial septum separates the lumina of the two adjacent Müllerian ducts (Fig. 6C). This midline septum largely disappears in the 9th week to form the midline uterovaginal canal, lined throughout with pseudostratified columnar Müllerian epithelium (Figs. 6E and 9) (Hunter, 1930; Koff, 1933).

The degree of midline Müllerian duct fusion is vastly different in humans versus mice. In humans the midline fusion is extensive, resulting in the midline uterovaginal canal and relatively short paired uterine tubes (Fig. 7). In contrast, in mice most of the Müllerian ducts remain separate (unfused), forming the paired oviducts and the large bilateral uterine horns. Only the caudal portions of the mouse

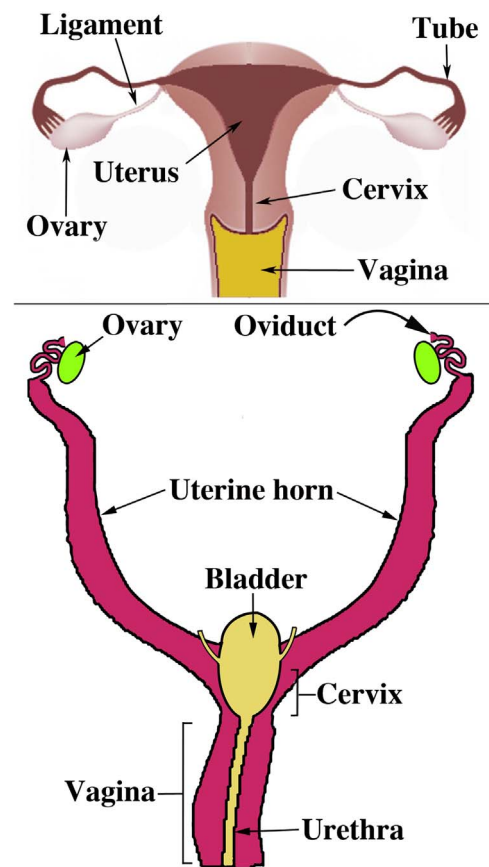


**Fig. 7.** Diagrams of human (A) and mouse (B) urogenital tracts emphasizing the marked difference in the degree of Müllerian duct fusion.

Müllerian ducts fuse to form the cervical canal and the so-called “Müllerian vagina” (discussed below) (Fig. 7).

### 3.2. Female reproductive tract development during the fetal period

The embryonic period transitions to the fetal period after the eighth gestational week. The book by Marjorie England provides a useful pictographic reference of intact human fetuses and dissections of human fetal reproductive tracts for the ninth week and beyond (England, 1983). In the following sections, we describe the development of the individual organs constituting the human female reproductive tract.

From a cytological perspective the epithelial cells of the embryonic Müllerian ducts and the uterovaginal canal are remarkably similar (Fig. 8). In the case of the uterovaginal canal (fused Müllerian ducts) the cells are pseudostratified columnar at all cranial-caudal levels, despite the fact that the epithelial cells of the uterovaginal canal will differentiate into the uterine corpus, uterine cervix and vagina, each having a unique and distinctive cytology. As indicated below, the determining factor in epithelial differentiation in the female reproductive tract is organ specific inductive clues from the surrounding mesenchyme.

#### 3.2.1. Uterine tube

The uterine tubes, originally called the Fallopian tubes, consist of 4 parts: (a) the funnel-shaped infundibulum with its finger-like projections (fimbria), (b) the ampulla where the oocyte is usually fertilized, (c) the isthmus, immediately lateral to the uterus, and (d) the intramural (or interstitial) portion within the uterine wall terminating in the uterotubal junction (Pauerstein et al., 1974). Information on development of the human uterine tube is scanty. The uterine tubes



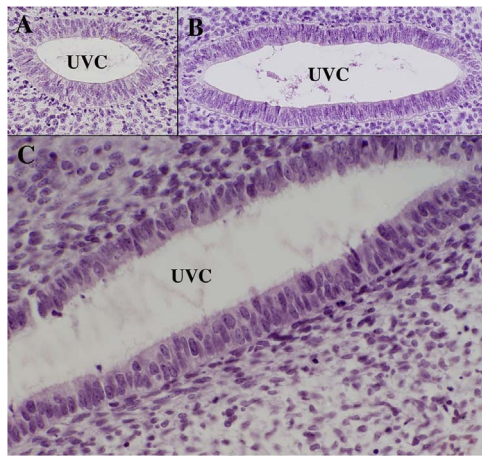


**Fig. 8.** High magnification images of the uterovaginal canal of an 8-week fetus stained with H & E. (A & B) are taken at cranial (A) and caudal (B) segments of the uterovaginal canal. (C) is also from a caudal domain and illustrates the pseudostratified nature of epithelium throughout the entire cranial-caudal extent of the uterovaginal canal at this stage.

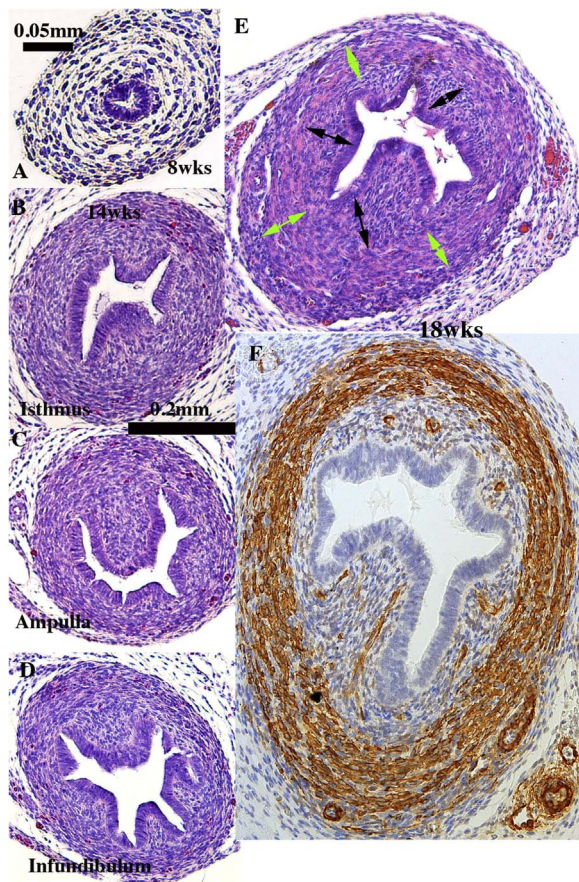


**Fig. 9.** Histologic sections of developing human uterine tubes. (A) Transverse section of that portion of an 8-week Müllerian duct destined to form the uterine tube. At this early stage the uterine tube consists of an undifferentiated simple columnar epithelium surrounded by loose mesenchyme. By 14 weeks, epithelial morphology of the isthmus (B), ampulla (C) and infundibulum (D) is more complex, and the stroma surrounding the epithelium is densely cellular (B–D). By the 18th week (E & F) the ampullary mesenchyme has differentiated into a condensed stromal layer (doubled-headed black arrows) associated with the epithelium and a surrounding circularly oriented layer (green double-headed arrows) that has differentiated into  $\alpha$ -actin-reactive smooth muscle (F). (A–E) = H & E, (F) =  $\alpha$ -actin.

develop from the paired cranial portions of the Müllerian ducts retained after the caudal segments fuse to form the midline uterovaginal canal. The fimbria develop from the irregular ostia of the Müllerian ducts into the abdominal cavity. At 8 weeks, the uterine tubes are narrow, and loose undifferentiated mesenchyme surrounds the epithelial ducts lined by a simple columnar epithelium (Fig. 9A). The epithelium of the earliest uterine tube that we have examined (8 weeks) discloses a single layer of a columnar epithelium (Fig. 8A). The cytoplasm is somewhat granular but without other distinguishing features. Two noticeable changes occur during the ensuing weeks to months: (a) The mucosa forms plicae, most prominently in the infundibulum and ampulla. This plication is less well developed in the isthmus and the uterine segment. By 14 weeks, a distinct gradient of mucosal plication is evident (Fig. 8B–D), which becomes more extreme as development proceeds. (b) Loose mesenchyme seen initially (Fig. 8A) differentiates into an inner dense stromal layer associated with the epithelium and outer circularly oriented layer (Fig. 9B–F). At 20 weeks,  $\alpha$ -actin-reactive smooth muscle is apparent throughout the uterine tube (Fig. 9F). In adulthood, the isthmus region is reported to contain an inner longitudinal smooth muscle layer, a middle circular layer, and an outer longitudinal layer (Pauerstein et al., 1974). The cell types typically seen in the tube of a mature adult woman are not seen during the fetal period. These include: ciliated cells, secretory cells (heavily granular cytoplasm and oval nucleus with its long axis parallel to the cell's long axis), intercalary or "peg" cells (with long slender dark nuclei compressed between adjoining cells).

### 3.2.2. Uterus corpus

The human uterine corpus undergoes remarkable changes during its development. The uterine corpus develops from the cranial portion of the midline uterovaginal canal, which formed as a result of fusion of the Müllerian ducts (Fig. 5). As the Müllerian ducts approach each other within the pelvis, they are initially separated by intervening mesenchyme, which subsequently disappears so that the basement membranes of the right and left Müllerian ducts come into direct contact. Finally, the intervening basement membranes disappear (Fig. 5D), and the epithelia of both Müllerian ducts fuse resulting initially in a midline epithelial septum (Fig. 5C–D) that is subsequently eliminated forming the midline uterovaginal canal (Figs. 5E and 10). The overall process bears considerable resemblance to events associated with the interaction of the Wolffian and Müllerian ducts during caudal migration of the Müllerian ducts (Fig. 3). The molecular mechanism by which the Müllerian ducts fuse is poorly understood. Based upon the human malformation, bicornuate uterus (Campbell, 1952; Davies and Walpole, 1949), it appears that Müllerian duct fusion begins caudally and progresses cranially. In any case, Koff's drawings show that length of the uterovaginal canal increases markedly during the course of development (Koff, 1933) (Fig. 10). This increased length likely reflects two separate processes: (a) A caudal to cranial "zipping together" of the bilateral Müllerian ducts, and (b) overall growth in length of the uterovaginal canal. Müllerian duct fusion requires further investigation.

The overall shape of the adult uterotubal junction and the lumen of the uterine corpus are unique (Figs. 2 and 11). Wholemound specimens photographed with transmitted light reveal epithelial contours within the uterovaginal canal (Figs. 2 and 11). The basic delta shape of the cranial portion of the uterovaginal canal (uterine corpus anlage) is recognizable by weeks 9–10, which subsequently expands and broadens (Figs. 2 and 11). Accordingly, transverse sections exhibit marked medial-lateral expansion of the uterovaginal canal cranially and less so caudally (Fig. 11G–H). The overall morphogenetic process surely involves growth in overall size and gradual shape change of the uterine lumen, which will continue to evolve until final adult morphology is achieved. The uterine corpus remains grossly undeveloped at parturi-

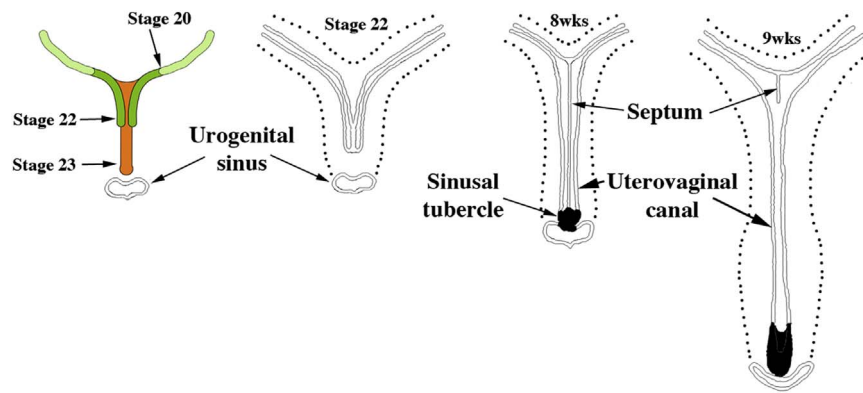


**Fig. 10.** Early Müllerian duct growth and fusion to form the midline uterovaginal canal. Length of the uterovaginal canal increases with developmental age. Adapted from Koff.

tion, undergoing considerable growth postnatally (Cooke et al., 2013). Functional and anatomical maturity is achieved at menarche.

**3.2.2.1. Uterine endometrium.** Through about the 16th week (Fig. 12), the body of the uterus is small (in comparison to the cervix and vagina) and is lined by a simple layer of columnar epithelial cells (Fig. 12D). Throughout all stages examined 8–21 weeks), the boundary between the uterine corpus and cervix cannot be discerned with certainty (Figs. 11–12). The rudimentary glands develop as shallow outpouchings also lined by a simple columnar epithelium. By 18 weeks, glands are elongated and branched within the endometrial stroma (Fig. 12E).

**3.2.2.2. Gland formation in the uterine corpus and uterine cervix.** Glands form within the developing uterine corpus and uterine cervix and initially appear at about 14–15 weeks (Fig. 12B–C). At this time the boundary between the uterine corpus and cervix

cannot be discerned with certainty. The rudimentary glands are shallow outpouchings lined by a simple columnar epithelium (Fig. 12D). Glands are initially found a considerable distance caudal to the uterine fundus, suggesting a regionality to gland formation. Indeed, the first glands to form are probably cervical glands. By 20 weeks uterine and cervical glands are elongated and branched within the stroma (Fig. 12E).

In the young adult, the endometrium discloses a basal region from which post-menstrual endometrial regeneration occurs following luminal endometrial shedding in every cycle. The early regenerative proliferation in the upper functional zone produces new straight to coiled glands that are relatively undifferentiated, have a relatively constant circular cross section and luminal diameter under 50  $\mu\text{m}$ . The cells lining the glands are columnar and have basally located nuclei. The stroma consists of spindly cells with relatively large nuclei and occasional mitoses (Dockery, 2002).

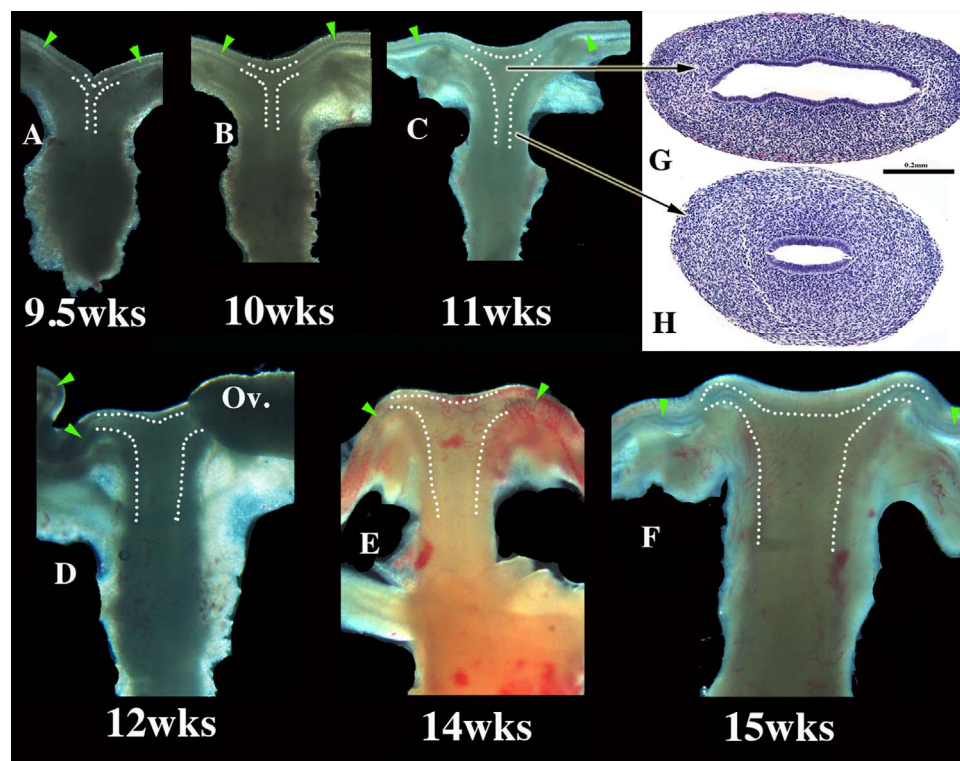


**Fig. 11.** Wholmount images of human fetal female reproductive tracts (A–F) photographed with transmitted light, and H & E stained transverse sections of the uterovaginal canal (G–H). Dotted lines indicate the contours of the uterotubal junction and the uterine cavity. Green arrowheads indicate the epithelium of the uterine tubes. Note the changing shape of the uterine lumen. The cranial portion is laterally expanded (G) and narrow caudally (H).



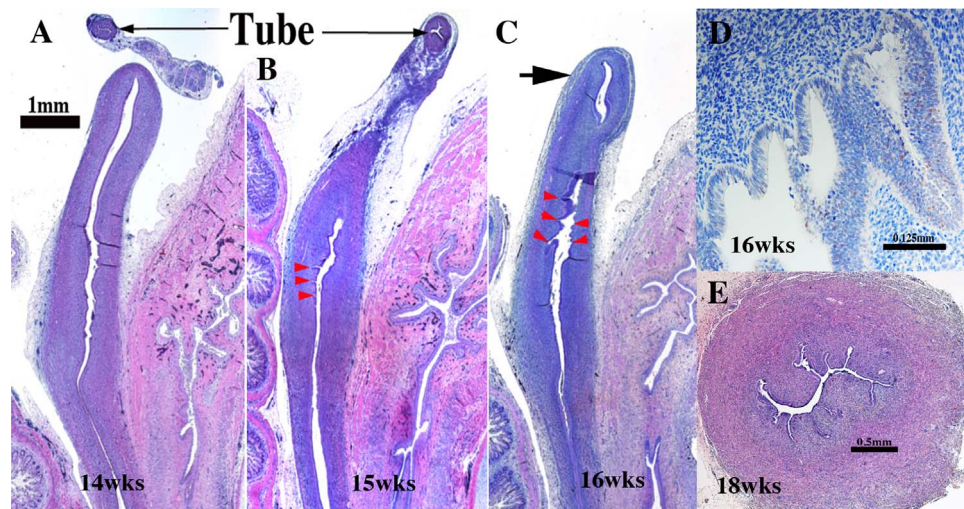


**Fig. 12.** Uterine/cervical glands (red arrowheads). Glands are rudimentary at 14 weeks (A), but can be seen by weeks 15 and 16 week (B & C). (D) The glands appear early on as shallow outpouchings of simple columnar epithelium. (E) By the 18th week, the uterine/cervical glands are elongated and branched. The fundus (C) is gland free (large arrow) at all ages examined, but appear later in development.

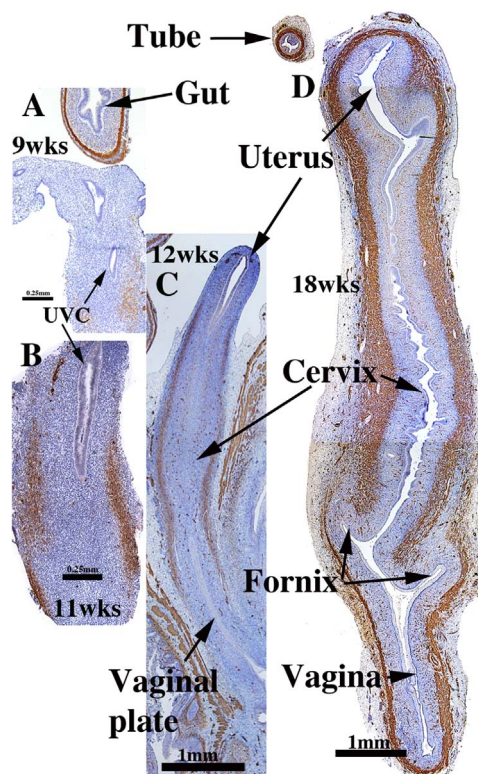


**Fig. 13.** α-Actin reactivity in human female reproductive tracts at (A) 9, (B) 11, (C) 12, and (D) 18 weeks. Faint α-actin reactivity first appears focally in mesenchyme of the 9-week uterovaginal canal, increasing in intensity by the 11 weeks. By 12 weeks α-actin reactivity is strong in the middle 2/4ths of the developing reproductive tract, and by 18 weeks, is strongly expressed through the developing female reproductive tract.

**3.2.2.3. Smooth muscle differentiation.** Faint α-actin reactivity, indicative of smooth muscle differentiation, was observed in the outer mesenchymal wall of the uterovaginal canal as early as 8–9 weeks of gestation (Fig. 13A). By the 11–12 week, the uterovaginal canal is well developed, and α-actin was detected most prominently in its middle 2/4<sup>ths</sup>, corresponding to the region of the presumptive cervix and upper vagina (Fig. 13B–C). At this time the mesenchymal wall of the uterine fundus and vagina showed negligible α-actin immunostaining. By the 20th week, all organs of the female reproductive tract displayed strong α-actin reactivity within their

fibromuscular walls, and by this time simple H&E staining revealed distinct myometrial development. Differentiation of α-actin-positive smooth muscle was consistently advanced and more prominent in the hindgut (Fig. 13A), urinary bladder and urethra (not illustrated) versus the female reproductive tract, suggesting that the timing of smooth muscle differentiation is organ specific during fetal life.

### 3.2.3. Uterine cervix

The cervix develops from the middle 2/4ths of the uterovaginal canal, consistent with the observation that the early fetal uterine cervix is about twice the length of the uterine corpus. Initially, the boundaries between the cervix and the uterine corpus as well as the between the cervix and vagina are unclear. Koff asserts that the cervix can be “recognized as a spindle-shaped thickening or condensation of the mesenchyme of the genital cord” in 8 to 10-week fetuses (Koff, 1933), a subtlety we find impossible to discern (Fig. 14A–C). At 18–20 weeks the vaginal fornices are recognizable (Fig. 14F) with the exocervix (also called ectocervix) projecting into the vagina. At earlier stages, however, the boundaries between the vagina, cervix and the uterine corpus remain imperceptible. For this reason, in “early stages” of cervical organogenesis we can only infer the cervical domain based upon cranial-caudal position with the uterovaginal canal, subtle changes of the endocervical contour in cross-section, and subtle histodifferentiation of the epithelium.

Initially, a simple columnar Müllerian epithelium lines the uterovaginal canal throughout (Figs. 5E and 8). During development, the “columnar epithelium lining the caudal portion of the uterovaginal canal becomes stratified” (Koff, 1933), an event our observations verify (Fig. 14D). According to Koff, at about 11 weeks “the conversion of columnar to stratified epithelium (within the uterovaginal canal) continues cranially until the transition between the two types becomes abrupt, a point which marks the junction of cervical and vaginal epithelium in the cervical canal” (Koff, 1933). This cervical-vaginal epithelial junction that Koff described at 11 weeks is transitory and reflects a squamo-columnar junction, which probably is not related to the definitive adult squamo-columnar junction at the transition between the endo- and exocervix. Koff states that the stratified epithelium of “the lower segment of the uterovaginal canal reaches its highest level at 100.5 mm (13 weeks)” which “marks the junction of the stratified and columnar epithelia in the cervical canal of the adult” (presumably the boundary between the endocervix and exocervix).



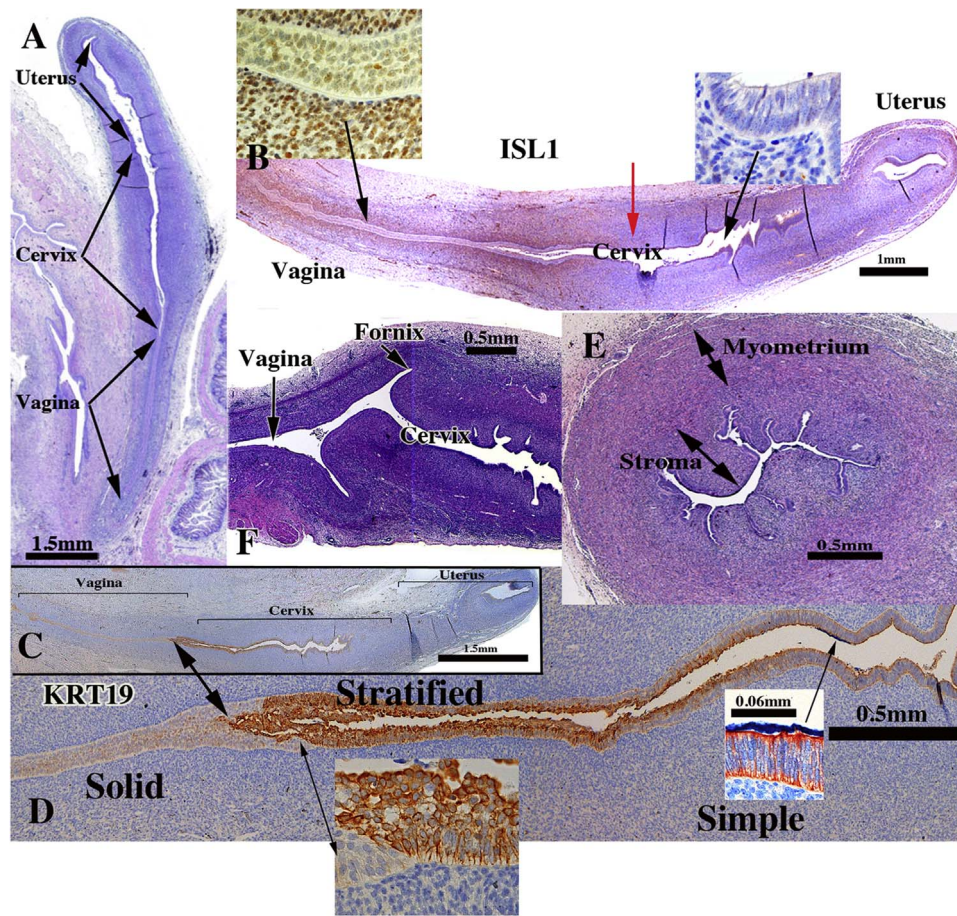


**Fig. 14.** Cervical development. (A–D) are sagittal sections of the female reproductive tract of a 16 week fetus (A=H & E stain, B=ISL1 immunostain, C–D=keratin 19 immunostain). Boundaries between the vagina, cervix and uterus are nebulous up to 18 weeks, when vaginal fornices become apparent (F). (B) ISL1 immunostaining is strong in vaginal stroma, absent in uterine stroma, with a sharp fall off in staining intensity at the mid-point of the uterovaginal canal (red arrow in B). Keratin 19 immunostaining (C–D) may also be indicative of vaginal-exocervical-endocervical boundaries. Cervical glands are prominent at 18 weeks of gestation (E).

While we have verified by histological observations most of Koff's assertions, his comments concerning boundaries between the cervix, uterine corpus and vagina are rather subtle, and his interpretations related to adult architecture are somewhat nebulous. Immunohistochemistry may help in defining vaginal-cervical-uterine boundaries. Immunostaining for ISL1 is promising in discerning the vaginal/cervical boundary, as ISL1 is enriched in vaginal mesenchyme, but not uterine mesenchyme (Gene Expression Omnibus (GEO) Series GSE44697) (Laronda et al., 2013) and Kurita (unpublished). ISL1 immunostaining is prominent in the developing vagina's mesenchyme (Fig. 14B and insets), but absent in the wall of the endocervix and uterine corpus. The steep reduction in ISL1 staining (Red arrow in Fig. 14B) may denote the cervical-vaginal boundary or future endocervical-exocervical boundary. KRT19 immunostaining (Fig. 14C–D and insets) revealed a sharp boundary between the KRT19-negative solid vaginal plate and KRT19-reactive stratified epithelium, which may denote the exocervical-vaginal boundary. Cranially the stratified KRT19-reactive stratified epithelium transitions to a KRT19-reactive simple columnar epithelium, which may denote the exocervical-endocervical boundary. These interpretations, while reasonable, require further attention. Glands are well developed within the cervix at 20 weeks of gestation (Fig. 14E).

The cervix of the adult nulliparous woman consists of the endocervix, which is continuous cranially with the uterine corpus and caudally with the exocervix that projects into the vaginal vault. The epithelium lining the adult cervix differentiates into a columnar mucinous epithelium, and with glands extending into the stroma. A stratified squamous epithelium, like that of the adult vagina, lines/

covers the exocervix. Normally the exocervix discloses no mucinous glands, although, in many women, there is some degree of ectropion, previously called eversion and erosion (Robboy et al., 1982b). In nulliparous women, the squamocolumnar junction that separates the exocervix from endocervix typically lies within the cervical canal slightly cranial to the cervix's external os (Burghardt, 1973).

### 3.2.4. Vagina

The debate regarding the origin of vaginal epithelium has remained of considerable interest ever since Johannes Müller described the duct that bears his name (Müllerian duct) (Müller, 1830). Various theories have suggested that vaginal epithelium receives contributions from epithelium of the urogenital sinus, Müllerian or Wolffian ducts alone or in combination (Koff, 1933; O'Rahilly, 1977; Forsberg, 1978; Bulmer, 1957). Particularly valuable are the recently published works of (Cai (2009); Fritsch et al. (2012, 2013).

Also in recent years, Kurita and Cunha have added another dimension to the story by showing the importance of mesenchymal-epithelial interactions in vaginal development and identifying key molecular mechanisms (Cunha, 1976; Kurita, 2010, 2011; Kurita et al., 2001, 2005; Terakawa et al., 2016). Using classic tissue recombination techniques, they showed that mouse vaginal mesenchyme plays a central role in vaginal epithelial differentiation by inducing and specifying vaginal epithelial cell fate and promoting vaginal epithelial differentiation (Cunha, 1976; Kurita et al., 2001). At least three growth factors (BMP4, Activin A, and FGF 7/10) produced by vaginal mesenchyme act in concert to elicit the expression of  $\Delta Np63$ , an isoform of p63, in the Müllerian epithelium (Terakawa et al., 2016)

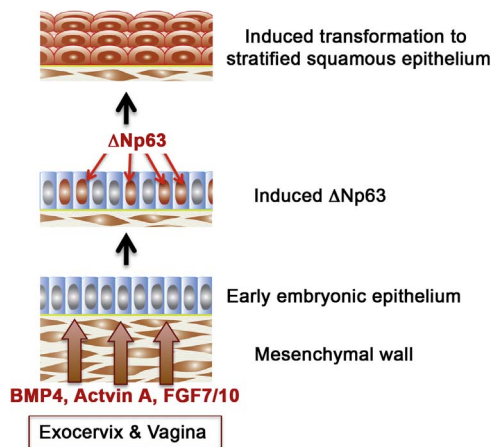


**Fig. 15.** Molecular mechanism of stratified squamous differentiation of vaginal epithelium. BMP4, actin A and FGF7/10 produced by vagina mesenchyme induce expression of p63 in Müllerian epithelium, which specifies and promotes vaginal epithelial differentiation.

(Fig. 15). Accordingly,  $\Delta Np63$  expression in Müllerian epithelium is subsequently followed by expression of keratin 14 and other vaginal epithelial differentiation markers. Significantly, in Müllerian duct epithelium-specific  $\Delta Np63$  null mice the vaginal epithelium remains columnar and exhibits a variety of uterine epithelial differentiation markers (Kurita et al., 2000; Laronda et al., 2013). Such findings show that  $\Delta Np63$  is critical for vaginal differentiation of Müllerian epithelium (Kurita et al., 2004). The central role of p63 appears to also apply to human vaginal epithelial differentiation (Kurita et al., 2005; Fritsch et al., 2012, 2013).

A novel experimental approach to examining the germ layer derivation of vaginal epithelium was to use transgenic mice in which the Müllerian, Wolffian or UGS epithelia were irreversibly labeled with an enhanced green fluorescent protein (EGFP) reporter (Kurita, 2010). The vaginal rudiment in mouse embryos and newborns consisting of the fused Müllerian ducts (Müllerian vagina) plus UGS epithelium (sinus vagina) were separately labeled red and green, respectively. However, postnatally the proportion of the sinus vagina was progressively reduced as the Müllerian vagina grew caudally. Indeed, by postpartum day 7, the Müllerian epithelium extended to the caudal end of the body, and the sinus vagina had retreated to the junction between the vagina and perineal skin. At puberty when the vagina opened, urogenital sinus epithelium was detected only in the vulva, and not in the vagina. Additionally, from embryonic to adult stages, residual Wolffian duct epithelium was only detected as remnants within the vaginal stroma, and not within vaginal or vulvar epithelium. Thus, in mice adult vaginal epithelium derives solely from Müllerian duct epithelium (MDE) (Kurita, 2010). Whether a similar process occurs in human vaginal development is the subject of this paper.

Koff's publication in 1933 and Bulmer's in 1957 are two most critical works examining the origin of the human vaginal epithelium (Bulmer, 1957; Koff, 1933). Koff proposed that vaginal epithelium derives from both Müllerian as well as urogenital sinus epithelium with Müllerian epithelium predominating. Bulmer states that the sinus upgrowth "forms the whole of (the vaginal) epithelial lining". These conclusions are based solely on hematoxylin and eosin (H & E) stained sections, which were reported as drawings and grey scale images. Most modern investigators access these data via low-resolution copies, making evaluation even more difficult. Fritsch et al. recently published in color, but the rather small in size of their published images hampers evaluation (Fritsch et al., 2012, 2013). Accordingly, we take this opportunity to review the relevant literature on vaginal epithelial differentiation, to provide large format color images of vaginal epithelial differentiation, and to utilize immunohistochemistry to explore the question of the relative contribution of Müllerian versus urogenital sinus epithelium to human vaginal epithelial differentiation.

The central player in human vaginal development is the uterovaginal canal formed via fusion of the right and left Müllerian ducts. Both Koff and Bulmer assert that the uterovaginal canal makes contact with the caudal aspect of the urogenital sinus in a region destined to form the urethra (Bulmer, 1957; Koff, 1933). Subsequently, epithelium of the uterovaginal canal with contributions from urogenital sinus epithelium (sinovaginal or sinus bulbs) form the "ribbon-like solid plate by two processes: (a) Stratification and fusion of the original cells lining the lumen (of the uterovaginal canal) and (b) lateral outgrowth. The sinus bulbs enlarge by the same process described above and their small cavities gradually become occluded. The epithelium between the two vaginal primordia, which are early distinguishable from each other, fuse insensibly to form the primitive vaginal plate" (Koff, 1933). Thus, both Koff and Bulmer agree that following initial contact of the uterovaginal canal with the UGS, the urogenital sinus epithelium proliferates and grows cranially as bilateral sinovaginal or sinus bulbs to contribute to the solid vaginal plate. The proposed upgrowth of sinus epithelium rests solely upon H & E-stained histological sections and led to the conclusion that the solid vaginal plate contains both Müllerian and urogenital sinus epithelial cells (Koff, 1933). Koff and Bulmer agree on this point but differ substantially about their interpretations of subsequent developmental events. Koff states that the cranial growth of the sinovaginal bulbs is limited, and thus definitive vaginal epithelium is 4/5ths Müllerian in origin with urogenital sinus epithelium contributing to only the caudal 1/5th of the vagina (Koff, 1933). Bulmer asserts that cranial growth of urogenital sinus epithelium displaces the Müllerian epithelium to the level of the exocervix, and thus proposes that human vaginal epithelium is exclusively derived from urogenital sinus epithelium (Bulmer, 1957). Clearly, the subtleties of epithelial differentiation inherent in H & E stained sections led these investigators to radically different conclusions regarding the derivation of human vaginal epithelium.

Advances in immunohistochemistry permit resolution of this developmental enigma. PAX2 is a protein expressed in Müllerian epithelium (Kurita, 2010), while FOXA1 is a protein expressed in endodermal urogenital sinus epithelium and its derivatives (Diez-Roux et al., 2011). Accordingly, PAX2 immunostaining was observed in the 8- to 9-week Müllerian duct, and subsequently in the uterovaginal canal, the uterine tube, uterine corpus, uterine cervix, but not in UGS derivatives such as the bladder and urethra (Fig. 16A–E). At 16 weeks FOXA1 immunostaining was observed in the urogenital sinus and its derivatives (bladder and urethra), but not in the Müllerian duct, the uterovaginal canal and its derivatives (uterine tube, uterine corpus, uterine cervix) (Fig. 16F). The strict dichotomy in immunostaining patterns with PAX2 and FOXA1 antibodies permits determination of the relative contribution of Müllerian and UGS sinus epithelia to the vaginal plate and, importantly and separately, to definitive vaginal epithelium.

The 12-week specimen provides an excellent starting point for investigating the relative contribution of Müllerian and urogenital sinus epithelia to human vaginal epithelium. At this stage the cranial (uterine) end of the uterovaginal canal has a lumen lined with a PAX2-reactive simple columnar epithelium (Fig. 17A). The caudal aspect of the uterovaginal canal is a solid vaginal plate composed of squamous cells. Its caudal end abuts the epithelium of the urethra/introitus (Fig. 17A and D). Nearly the entire vaginal plate is PAX2-reactive (Fig. 17A–B). Only its most caudal portion of the vaginal plate is FOXA1-reactive (Fig. 17C). During the next several weeks (14–16 weeks), the solid vaginal plate increases in extent, now constituting about 1/3rd of the developing female reproductive tract's total length (Fig. 18A and D). This additional new growth appears to be derived solely from FOXA1-reactive epithelial cells (Fig. 18C and D) and not PAX2-reactive epithelial cells (Fig. 18A and B).

According to Koff, the vaginal plate begins to cavitate by the 16th week (151 mm) and by the 19th week (162 mm) is mostly complete (Koff, 1933). Vaginal fornices are certainly well defined at 18 weeks of



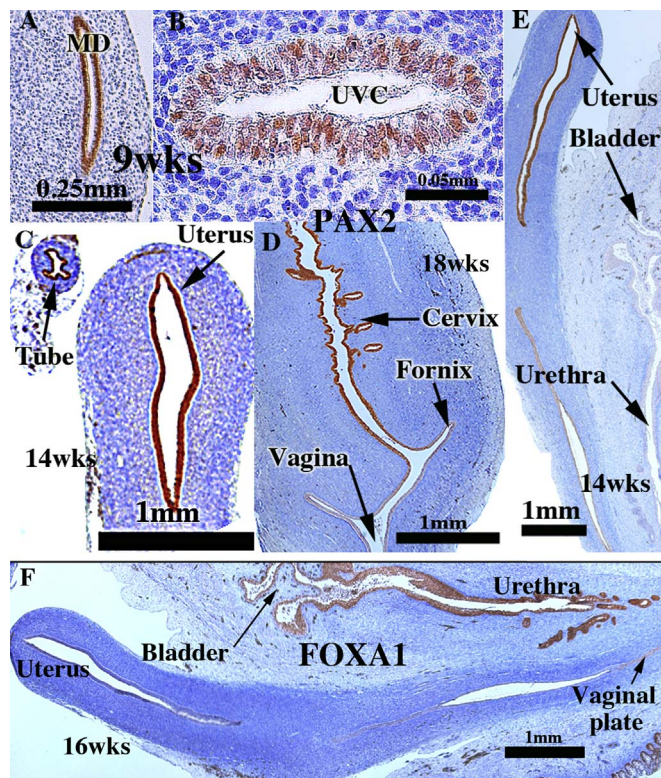


**Fig. 16.** PAX2 (A–E) and FOXA1 (F) immunostaining of human female fetal reproductive tracts at the ages indicated. PAX2 is expressed in the Müllerian duct and uterovaginal canal at 9 weeks (A–B), and in epithelium of the uterine tube, uterus and cervix (C–E). FOXA1 is expressed only in UGE derivatives (urethra and bladder) (F).

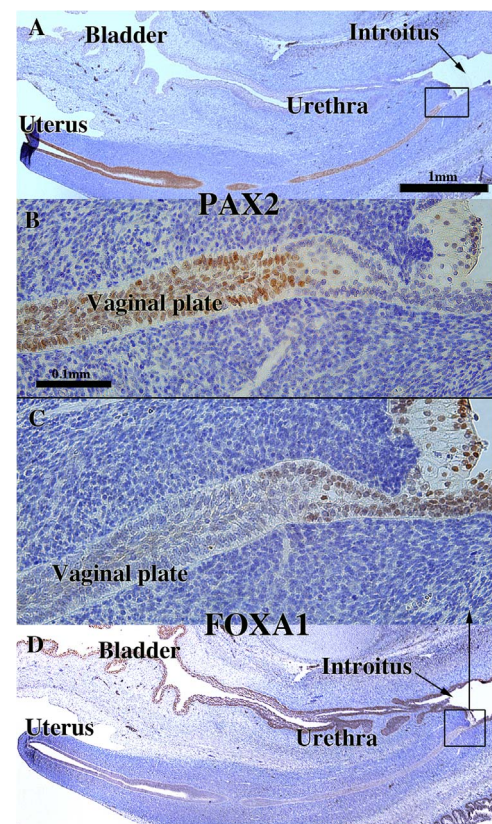


**Fig. 17.** Sagittal sections of a 12-week human female fetal reproductive tract immunostained with PAX2 (A–B) and FOXA1 (C–D). PAX2-reactive epithelial cells extend to near the junction with the introitus/urethra (A–B). FOXA1-reactive epithelial cells extend only a short distance into the solid vaginal plate (C–D). Scale bar in A also refers to D. Scale bar in D also refers to C.

gestation with the exocervix projecting into the vaginal vault (Figs. 14F and 19A and D). PAX2-reactive Müllerian epithelium appeared was detected in the epithelium of the uterine tube, uterine corpus, uterine cervix, and the upper (cranial) portion of the vagina. The lumen of the lower (caudal) vagina was lined with FOXA1-reactive epithelial cells (Fig. 19C–D). An important caveat regarding Fig. 19 is that the lower aspect of the vagina is not present. Accordingly, a completely intact 21-week specimen was examined which contained the entire female reproductive tract from the vaginal introitus to the uterus (Fig. 20). The vaginal epithelium exhibited estrogenic stimulation throughout and was many cell layers thick. Endogenous estrogen levels are known to elevate late in the second and especially in the third trimester (Oakey, 1970). Epithelial FOXA1 staining was observed from the introitus to the cervix. The vaginal fornices that were evident at 18 weeks (Fig. 19) were “filled in” (Fig. 20B) presumably by epithelial proliferation. Epithelial PAX2 immunostaining was observed from the cervix (Fig. 20D) to the uterus (not illustrated). The abrupt change in FOXA1/PAX2 staining occurred at the same point in adjacent sections (Fig. 20C, E, F). These data support Bulmer’s proposal that the entire vaginal epithelium is derived from urogenital sinus epithelium, even though examination of later stages, perhaps to term, would be a helpful addition.

The cranial expansion of the vaginal plate, and especially the contribution of FOXA1-reactive urogenital sinus epithelial cells to the vaginal plate, deserves comment/speculation. The cranial expansion of the solid vaginal plate from 12 to 16 weeks seen in sagittal sections was verified in serial transverse sections of 14-, 15- and 16-week specimens. Most of the vaginal plate at this stage was PAX2-negative and FOXA1-positive (Fig. 21A–B). However, at the most cranial region of the vaginal plate, occasional FOXA1-reactive cells were seen flanked

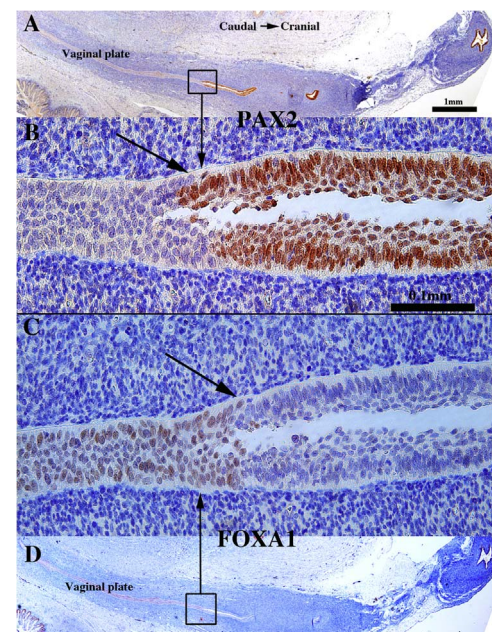


**Fig. 18.** Sagittal sections of a 16-week human female fetal reproductive tract immunostained with PAX2 (A–B) and FOXA1 (C–D). FOXA1-reactive epithelial cells form all of the solid vaginal plate (C–D). PAX2-reactive epithelial cells constitute a stratified epithelium lining the lumen of the uterovaginal canal (A–B). Scale bar in A also refers to D. Scale bar in D also refers to C.



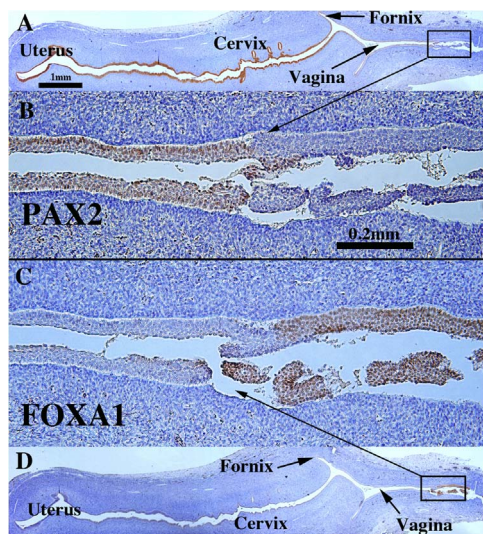


**Fig. 19.** Sagittal sections of an 18-week human female fetal reproductive tract immunostained with PAX2 (A–B) and FOXA1 (C–D). PAX2-reactive epithelial cells line the lumen of the female reproductive tract from the uterine tube to the cranial aspect of the vagina (A–B). PAX2 staining is present, but weak in vaginal epithelium (B). FOXA1-reactive epithelial cells line the lower (caudal) vagina (C–D). Scale bar in A also refers to D. Scale bar in D also refers to C.

the PAX2-reactive cells (Fig. 21C–D). Thus, both sagittal and transverse sections verify that the PAX2/FOXA1 boundary moved cranially over the period of 12–16 weeks as the vaginal plate lengthened in its overall cranial-caudal dimension. Our observations support Koff and Bulmer that over the period of 12–16 weeks the Müllerian-urogenital sinus epithelial boundary moves cranially as the vaginal plate increased its cranial-caudal dimension in large part due to cranial expansion of the UGE (Koff, 1933; Bulmer, 1957).

The mechanism by which the cranial shift in the PAX2/FOXA1 boundary within the vaginal plate occurs at this time remains unknown. But our observation that small isolated islands of PAX2-reactive cells were surrounded in entirety by FOXA1-reactive cells (Fig. 21E–H) deserves special attention and supports Bulmer's belief (1957) that the vagina forms when the UGS epithelium displaces (eliminates) the native Müllerian epithelial cells. These small islands of PAX2-reactive Müllerian epithelial cells were observed in various cranial-caudal positions within the vaginal plate, from the junction with the introitus to various cranial positions. This observation indicates that PAX2-reactive Müllerian epithelial cells originally (12 weeks) extended to near the introitus (Fig. 17) and have been displaced/eliminated as the FOXA1-reactive UGE cells advanced cranially such that only small isolated islands of PAX2-reactive cells remained within the vaginal plate (Fig. 21E–H). These isolated islands of Müllerian duct epithelium that were retained within the epithelial layers, but not attached to the basement membrane likely reflect the ongoing process whereby FOXA1-reactive cells undermine and force the sloughing/displacement of the residual Müllerian epithelial cells. The potential retention of PAX2-reactive islands of Müllerian epithelial cells on the basement membrane (not seen in our series) may explain the aberrant, occasional finding of embryonic type glands in the vagina of young women (Robboy et al., 1986).

Our observations support many of Bulmer's observations. For example, “the caudal end of the Müllerian tissue is embedded in the cranial end of the sinus upgrowth” (Bulmer, 1957). Regarding displacement of Müllerian epithelium, “the sinus epithelium gradually extended further and further cranially until eventually the Müllerian epithelium was completely displaced from the vaginal plate” (Bulmer, 1957). While our observations support displacement/elimination of Müllerian epithelium by the upgrowth of UGE, other mechanistic

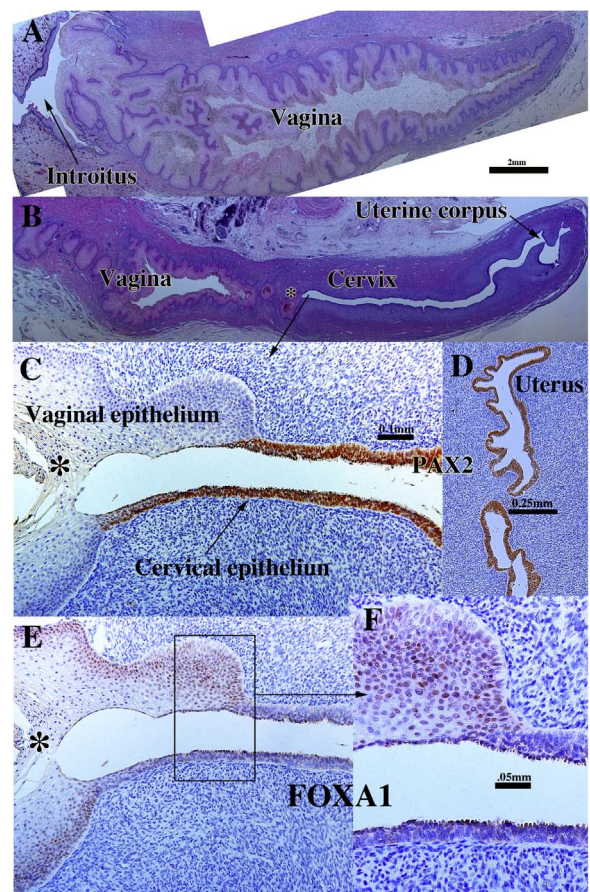


**Fig. 20.** Sagittal sections of a 21-week female reproductive tract. Due to section orientation (A depicts the lower portion of the specimen (introitus to upper vagina), and (B) depicts the upper portion of the specimen (vagina, cervix and uterus) via H & E stain. The vaginal epithelium is many layers thick due to estrogenic stimulation (A–B). In (B) note the abrupt transition in epithelial differentiation at the vaginal/cervical border. PAX2 staining of the vaginal/cervical border (C) shows prominent PAX2 immunostaining of stratified but relatively thin cervical epithelium (indicative of Müllerian duct origin) and PAX2-negative vaginal epithelium (C). Epithelium of the uterine corpus (D) is strongly PAX2-reactive. FOXA1 immunostaining was seen uniformly throughout the entire vagina, and FOXA1 immunostaining abruptly stopped at the vaginal/cervical border (E–F) in mirror image to PAX2 immunostaining (C).

scenarios are possible requiring further research. Also, since the oldest specimen analyzed in our study came from a 21-week fetus, further changes in the relative contribution MDE versus UGE to human vaginal epithelium may occur at later stages.

#### 4. Discussion

Investigation of developing human organs, including the female reproductive tract, is severely limited by the availability of human embryonic and fetal specimens, and a complete developmental sequence requires specimens from all 3 trimesters up to and including birth. Such comprehensive collections are difficult for any single group to obtain. Consequently, studies will be limited by the ages of specimens available. The specimens in our study ranged from 5 to 21 weeks of gestation. In our study additional specimens, particularly in the 16–21 week range, need to be examined in the future. Also developmental events post-21 weeks need to be examined. Availability of a broader series of specimens could add additional important information, especially on vaginal epithelial differentiation.

With this caveat, we have re-visited the classic studies of Koff and Bulmer and extended the more recent studies of Fritsch et al. by providing detailed high-resolution documentation of human female



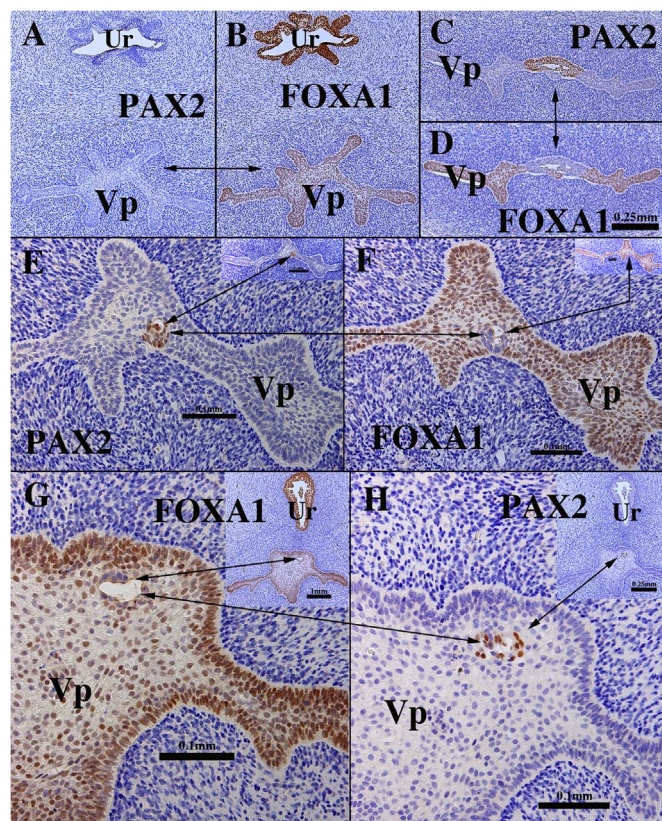


**Fig. 21.** Transverse sections of the vaginal plate of 14- (A–F) and 16-week (G–H) female fetuses. Most of the vaginal plate (Vp) is PAX2-negative (A) and FOXA1-positive (B). In the cranial portion of the vaginal plate (C–D) a remnant of PAX2-positive Müllerian epithelium can be seen. Scattered at various cranial-caudal levels small islands of PAX2-positive islands are seen (E–H). Note “mirror images” of PAX2 and FOXA1 immunostaining. The urethra (Ur) is FOXA1-positive and PAX2-negative.

reproductive tract development (Bulmer, 1957; Fritsch et al., 2012, 2013; Koff, 1933). Significantly, through use of immunohistochemistry we have described the dynamic age-dependent changes in the contribution of Müllerian versus UGS epithelium in the development of human vaginal epithelium, which depart markedly from the complete elimination of UGS epithelial cells from vaginal epithelium in mice (Kurita, 2010). Of course, one must be mindful of the fact that such studies in mice encompassed embryonic through adult stages (Kurita, 2010), and our study extended to only week 21 of gestation. Thus, additional older human specimens will be required to complete the story.

While our immunohistochemical studies support Bulmer's proposal that during development of the human vagina, urogenital sinus epithelium of the vaginal plate grows cranially to completely replace Müllerian, cell lineage-tracing is the only method to definitively determine the relative contribution of Müllerian versus UGS epithelium in the development of vaginal epithelium. Such an approach is impossible in humans. Immunohistochemistry of “lineage markers” has been used previously with the tacit assumption that lineage markers are stable relative to developmental stage and differentiation status. In this study we have used FOXA1 as a marker of endoderm, based upon the report FOXA1 protein expression in urogenital sinus epithelium and its derivatives (Diez-Roux et al., 2011). Consistent with this idea is our finding of FOXA1 reactivity in epithelium of the bladder, urethra, upper anus and rectum, even though FOXA1 is also known to be expressed in other developing tissues (Carlsson and Mahlapuu, 2002; Besnard et al., 2004). We used PAX2 as a marker of Müllerian epithelium based upon its prior use for this purpose in mouse vaginal development (Kurita, 2010). Our choice of PAX2 and

FOXA1 as markers of Müllerian and urogenital sinus epithelia were dictated by the literature cited above and the availability of useful antibodies. Immunostaining patterns observed in this study were entirely consistent with the known distribution of Müllerian and urogenital sinus epithelia early in human female reproductive tract development and consistent with Bulmer's view that urogenital sinus epithelium grows cranially to completely replace the Müllerian epithelium (Bulmer, 1957). However, another possibility is that the Müllerian epithelium is induced by the surrounding stroma to change marker expression (PAX2 to FOXA1 transition) based upon animal studies showing that stroma determines expression of cell fate markers in the vaginal epithelium (Cunha, 1976; Kurita et al., 2001). This possibility is unlikely based upon unpublished data in which tissue recombinants were prepared with mouse vaginal stroma and human uterine tube epithelium (Cunha and Cao, unpublished). The mouse vaginal stroma was obtained from early neonatal mice when the vaginal epithelium contained both urogenital sinus and Müllerian epithelia. In such tissue recombinants the human uterine tubal epithelium was induced to differentiate into stratified squamous differentiation and express vaginal epithelial markers while continuing to maintain expression of PAX2 without co-expression of FOXA1. FOXA1/FOXA2 are pioneer transcription factors essential for the function of steroid receptors based upon studies of mutant mice and human cancer cells (Augello et al., 2011; Bernardo and Keri, 2012; Kaestner, 2010). However, given the critical role of estrogen and progesterone in the cervix and vagina, is it possible that human fetal Müllerian epithelium can turn on FOXA1 as they differentiate/mature into a stratified squamous epithelium? Thus, the relationship between estrogenic response and FOXA1 expression in the developing human vagina needs further examination, especially in specimens in the 18–21 week range when human fetal vaginal epithelium proliferates into a thick relatively mature vaginal epithelium.

In the course of our studies, several events were identified requiring further investigation both in human and mouse urogenital development. A particularly intriguing problem is the mechanism of Müllerian duct fusion, which in humans results in formation of the uterovaginal canal and in mice results in formation of the cervical canal and the “Müllerian vagina”. Another interesting issue concerns the boundaries between the developing human vagina, cervix and uterine corpus, which are for the most part imperceptible during development. Thus, organ-specific markers would be extremely valuable and might clarify another fascinating developmental question concerning the formation of glands penetrating within the uterine corpus and uterine cervix. Our observations show that the glands of the uterine cervix appear much earlier than glands of the uterine corpus. Is there a regionality to gland development within the developing human female reproductive tract? Additionally, there is the question of the relevance/applicability of animal models to human development. The tacit, but mostly unproven, idea is that animal models are faithful surrogates of human development. This idea appears to be true for many developmental events, but clearly does not apply across the board. It is essential, whenever possible, to understand those developmental processes that are fundamentally similar/identical in humans and mice, and just as important, those development events that differ substantially in these two species. Human and mouse vaginal development differ significantly in many respects. Finally, this paper provides an important trove of information that will be useful in understanding the pathogenic effect of exogenous estrogens such as diethylstilbestrol, bisphenol A and many others on the developing female reproductive tract. The two companion papers, especially the third in this series, directly address this issue.

## Acknowledgements

This study was supported by NIH grant DK058105 to Dr. Baskin and R01 CA154358 to Dr. Kurita. The authors appreciate the superb technical expertise of Mei Cao.



## References

- Augello, M.A., Hickey, T.E., Knudsen, K.E., 2011. FOXA1: master of steroid receptor function in cancer. *EMBO J.* 30, 3885–3894.
- Bernardo, G.M., Keri, R.A., 2012. FOXA1: a transcription factor with parallel functions in development and cancer. *Biosci. Rep.* 32, 113–130.
- Besnard, V., Wert, S.E., Hull, W.M., Whitsett, J.A., 2004. Immunohistochemical localization of Foxa1 and Foxa2 in mouse embryos and adult tissues. *Gene Expr. Pattern.* 5, 193–208.
- Bulmer, D., 1957. The development of the human vagina. *J. Anat.* 91, 490–509.
- Burghardt, E., 1973. Early histological diagnosis of cervical cancer. *Major Probl. Obstet. Gynecol.* 6, 1–401.
- Cai, Y., 2009. Revisiting old vaginal topics: conversion of the Mullerian vagina and origin of the "sinus" vagina. *Int. J. Dev. Biol.* 53, 925–934.
- Campbell, J.G., 1952. Bicornuate uterus. *Can. Med. Assoc. J.* 67, 355–356.
- Carlsson, P., Mahlapuu, M., 2002. Forkhead transcription factors: key players in development and metabolism. *Dev. Biol.* 250, 1–23.
- Cooke, P.S., Spencer, T.E., Bartol, F.F., Hayashi, K., 2013. Uterine glands: development, function and experimental model systems. *Mol. Hum. Reprod.* 19, 547–558.
- Cunha, G.R., 1976. Stromal induction and specification of morphogenesis and cytodifferentiation of the epithelia of the Mullerian ducts and urogenital sinus during development of the uterus and vagina in mice. *J. Exp. Zool.* 196, 361–370.
- Cunha, G.R., Kurita, T., Cao, M., Shen, J., Robboy, S., Baskin, L., 2017a. Molecular mechanisms of development of the human fetal female reproductive tract. *Differentiation*, (In Press).
- Cunha, G.R., Kurita, T., Cao, M., Shen, J., Robboy, S.J., Baskin, L., 2017b. Estrogenic response in developing human female reproductive tract xenografts grown in athymic mouse hosts. *Differentiation*, (In press).
- Cunha, G.R., Taguchi, O., Namikawa, R., Nishizuka, Y., Robboy, S.J., 1987. Teratogenic effects of Clomid, tamoxifen, and diethylstilbestrol on the developing human female genital tract. *Hum. Pathol.* 18, 1132–1143.
- Davies, W.M., Walpole, G.R., 1949. Bicornuate uterus. *Med. J. Aust.* 2, 166.
- Diez-Roux, G., Banfi, S., Sultan, M., Geffers, L., Anand, S., Rozado, D., Magen, A., Canidio, E., Pagani, M., Peluso, I., Lin-Marq, N., Koch, M., Bilio, M., Cantiello, I., Verde, R., De Masi, C., Bianchi, S.A., Cicchini, J., Perroud, E., Mehmeti, S., Dagand, E., Schrinner, S., Nurnberger, A., Schmidt, K., Metz, K., Zwingmann, C., Brieske, N., Springer, C., Hernandez, A.M., Herzog, S., Grabbe, F., Sieverding, C., Fischer, B., Schrader, K., Brockmeyer, M., Dettmer, S., Helbig, C., Alunni, V., Battaini, M.A., Mura, C., Henrichsen, C.N., Garcia-Lopez, R., Echevarria, D., Puelles, E., Garcia-Calero, E., Kruse, S., Uhr, M., Kauck, C., Feng, G., Milyaev, N., Ong, C.K., Kumar, L., Lam, M., Semple, C.A., Gyenesei, A., Mundlos, S., Radelof, U., Lehrach, H., Sarmientos, P., Raymond, A., Davidson, D.R., Dolle, P., Antonarakis, S.E., Yaspo, M.L., Martinez, S., Baldock, R.A., Eichele, G., Ballabio, A., 2011. A high-resolution anatomical atlas of the transcriptome in the mouse embryo. *PLoS Biol.* 9, e1000582.
- Dockery, P., 2002. The fine structure of the mature human endometrium. In: Glasser, S.R., Aplin, J.D., Giudice, L.C., Tabibzadeh, S. (Eds.), *The Endometrium*. Taylor & Francis, London.
- Drey, E.A., Kang, M.S., McFarland, W., Darney, P.D., 2005. Improving the accuracy of fetal foot length to confirm gestational duration. *Obstet. Gynecol.* 105, 773–778.
- England, M.A., 1983. *Color Atlas of Life Before Birth: Normal Fetal Development*. Year Book Medical Publishers, Chicago.
- Forsberg, J.G., 1973. Cervicovaginal epithelium: its origin and development. *Am. J. Obstet. Gynecol.* 115, 1025–1043.
- Forsberg, J.G., 1978. Development of the human vaginal epithelium. In: Hafez, E.S.E., Evans, T.N. (Eds.), *The Human Vagina*. Elsevier, No. Holland, New York, 3–20.
- Forsberg, J.G., 1996. A morphologist's approach to the vagina. *Acta Obstet. Gynecol. Scand. Suppl.* 163, 3–10.
- Fritsch, H., Hoermann, R., Bitsche, M., Pechriggl, E., Reich, O., 2013. Development of epithelial and mesenchymal regionalization of the human fetal utero-vaginal anlagen. *J. Anat.* 222, 462–472.
- Fritsch, H., Richter, E., Adam, N., 2012. Molecular characteristics and alterations during early development of the human vagina. *J. Anat.* 220, 363–371.
- Frutiger, P., 1969. Zur Fruhentwicklung der Ductus paramesonephrici und des Mullerschen Hügels beim Menschen. *Acta Anat.* 72, 233–245.
- Gruenewald, P., 1941. The relation of the growing Mullerian duct to the Wolffian duct and its importance for the genesis of malformations. *Anat. Rec.* 81, 1–19.
- Hunter, R.H., 1930. Observations on the development of the human female genital tract. *Contr. Embryol. Carneg.* Inst. 22, 91–108.
- Kaestner, K.H., 2010. The FoxA factors in organogenesis and differentiation. *Curr. Opin. Genet. Dev.* 20, 527–532.
- Kobayashi, A., Kwan, K.M., Carroll, T.J., McMahon, A.P., Mendelsohn, C.L., Behringer, R.R., 2005. Distinct and sequential tissue-specific activities of the LIM-class homeobox gene *Lim1* for tubular morphogenesis during kidney development. *Development* 132, 2809–2823.
- Koff, A.K., 1933. Development of the vagina in the human fetus. *Contrib. Embryol. Carnegie Inst. Wash.* 24, 59–90.
- Konishi, I., Fujii, S., Okamura, H., Mori, T., 1984. Development of smooth muscle in the human fetal uterus: an ultrastructural study. *J. Anat.* 139, 239–252.
- Kurita, T., 2010. Developmental origin of vaginal epithelium. *Differ. Res. Biol. Divers.* 80, 99–105.
- Kurita, T., 2011. Normal and abnormal epithelial differentiation in the female reproductive tract. *Differ. Res. Biol. Divers.* 82, 117–126.
- Kurita, T., Cooke, P.S., Cunha, G.R., 2001. Epithelial-stromal tissue interaction in paramesonephric (Mullerian) epithelial differentiation. *Dev. Biol.* 240, 194–211.
- Kurita, T., Cunha, G.R., Robboy, S.J., Mills, A.A., Medina, R.T., 2005. Differential expression of p63 isoforms in female reproductive organs. *Mech. Dev.* 122, 1043–1055.
- Kurita, T., Lee, K.-J., Cooke, P.S., Lydon, J.P., Cunha, G.R., 2000. Paracrine regulation of epithelial progesterone receptor and lactoferrin by progesterone in the mouse uterus. *Biol. Reprod.* 62, 831–838.
- Kurita, T., Mills, A.A., Cunha, G.R., 2004. Roles of p63 in the diethylstilbestrol-induced cervicovaginal adenosis. *Development* 131, 1639–1649.
- Laronda, M.M., Unno, K., Ishi, K., Serna, V.A., Butler, L.M., Mills, A.A., Orvis, G.D., Behringer, R.R., Deng, C., Sinha, S., Kurita, T., 2013. Diethylstilbestrol induces vaginal adenosis by disrupting SMAD/RUNX1-mediated cell fate decision in the Mullerian duct epithelium. *Dev. Biol.* 381, 5–16.
- Li, Y., Sinclair, A., Cao, M., Shen, J., Choudhry, S., Botta, S., Cunha, G., Baskin, L., 2015. Canalization of the urethral plate precedes fusion of the urethral folds during male penile urethral development: the double zipper hypothesis. *J. Urol.* 193, 1353–1359.
- Mercer, B.M., Sklar, S., Shariatmadar, A., Gillieson, M.S., D'Alton, M.E., 1987. Fetal foot length as a predictor of gestational age. *Am. J. Obstet. Gynecol.* 156, 350–355.
- Mhaskar, R., Agarwal, N., Takkar, D., Buckshee, K., Anandalakshmi, Deorari, A., 1989. Fetal foot length—a new parameter for assessment of gestational age. *Int. J. Gynaecol. Obstet.* 29, 35–38.
- Müller, J., 1830. *Bildungsgeschichte der Genitalien*. Arnz, Dusseldorf.
- Mutter, G.L., Robboy, S.J., 2014. Embryology. In: Mutter, G.S., Prat, J. (Eds.), *Pathology of the Female Reproductive Tract*. Churchill Livingstone, London, 1–17.
- O'Rahilly, R., 1973. The embryology and anatomy of the uterus. In: Norris, H.J., Hertig, A.T., Abell, M.R. (Eds.), *The Uterus*. Williams and Wilkins Co, Baltimore, 17–39.
- O'Rahilly, R., 1977. Prenatal human development. In: Wynn, R.M. (Ed.), *Biology of the Uterus*. Plenum Press, New York, 35–57.
- O'Rahilly, R., 1983. The timing and sequence of events in the development of the human reproductive system during the embryonic period. *Anat. Embryol.* 166, 247–261.
- O'Rahilly, R., Muller, F., 1992. The reproductive system. In: O'Rahilly, R., Muller, F. (Eds.), *Human Embryology and Teratology*. Wiley-Liss, New York, 207–224.
- O'Rahilly, R., Muller, F., 2010. Developmental stages in human embryos: revised and new measurements. *Cells Tissues Organs* 192, 73–84.
- Oakey, R.E., 1970. The progressive increase in estrogen production in human pregnancy: an appraisal of the factors responsible. *Vitam. Horm.* 28, 1–36.
- Pauerstein, C.J., Hodgson, B.J., Kraman, M.A., 1974. The anatomy and physiology of the oviduct. *Obstet. Gynecol. Annu.* 3, 137–201.
- Reich, O., Fritsch, H., 2014. The developmental origin of cervical and vaginal epithelium and their clinical consequences: a systematic review. *J. Low. Genit. Tract. Dis.* 18, 358–360.
- Robboy, S.J., Bentley, R.C., Russell, P., 2002. Embryology and disorders of abnormal sexual development. In: Robboy, S.J., Anderson, M., Russell, P. (Eds.), *Pathology of the Female Reproductive Tract*. Churchill Livingstone, London.
- Robboy, S.J., Hill, E.C., Sandberg, E.C., Czernobilsky, B., 1986. Vaginal adenosis in women born prior to the diethylstilbestrol era. *Hum. Pathol.* 17, 488–492.
- Robboy, S.J., Mutter, G.L., 2014. Disorders of sexual development. In: Mutter, G.S., Prat, J. (Eds.), *Pathology of the Female Reproductive Tract*. Churchill Livingstone, London, 18–47.
- Robboy, S.J., Taguchi, O., Cunha, G.R., 1982a. Normal development of the human female reproductive tract and alterations resulting from experimental exposure to diethylstilbestrol. *Hum. Pathol.* 13, 190–198.
- Robboy, S.J., Welch, W.R., Young, R.H., Truslow, G.Y., Herbst, A.L., Scully, R.E., 1982b. Topographic relation of cervical ectropion and vaginal adenosis to clear cell adenocarcinoma. *Obstet. Gynecol.* 60, 546–551.
- Rodriguez, E., Jr., Weiss, D.A., Ferretti, M., Wang, H., Menshenia, J., Risbridger, G., Handelsman, D., Cunha, G., Baskin, L., 2012. Specific morphogenetic events in mouse external genitalia sex differentiation are responsive/dependent upon androgens and/or estrogens. *Differ. Res. Biol. Divers.* 84, 269–279.
- Shapiro, E., Huang, H.Y., Wu, X.R., 2000. Uroplakin and androgen receptor expression in the human fetal genital tract: insights into the development of the vagina. *J. Urol.* 164, 1048–1051.
- Sinisi, A.A., Pasquali, D., Notaro, A., Bellastella, A., 2003. Sexual differentiation. *J. Endocrinol. Investig.* 26, 23–28.
- Smith, B., 2016. *The Multi-Dimensional Human Embryo*. University of Michigan, Ann Arbor, MI.
- Streeter, G.L., 1951. Developmental horizons in human embryos. Age groups XI to XXIII. Carnegie Institution of Washington, Washington DC.
- Sulak, O., Cosar, F., Malas, M.A., Cankara, N., Cetin, E., Tagil, S.M., 2007. Anatomical development of the fetal uterus. *Early Hum. Dev.* 83, 395–401.
- Taguchi, O., Cunha, G.R., Lawrence, W.D., Robboy, S.J., 1984. Timing and irreversibility of Mullerian duct inhibition in the embryonic reproductive tract of the human male. *Dev. Biol.* 106, 394–398.
- Taguchi, O., Cunha, G.R., Robboy, S.J., 1983. Experimental study of the effect of diethylstilbestrol on the development of the human female reproductive tract. *Int. J. Biol. Res. Pregnancy* 4, 56–70.
- Terakawa, J., Rocchi, A., Serna, V.A., Bottinger, E.P., Graff, J.M., Kurita, T., 2016. FGFR2IIIb-MAPK activity is required for epithelial cell fate decision in the lower Mullerian duct. *Mol. Endocrinol.* 30, 783–795.